THE ASTROPHYSICAL JOURNAL, 240:L121–L125, 1980 September 15


# TIME-RESOLVED IMAGING AND SPECTRAL STUDIES OF AN X-RAY BURST FROM THE GLOBULAR CLUSTER TERZAN 2

J. E. GRINDLAY,[1] H. L. MARSHALL, P. HERTZ, AND A. SOLTAN[2]
Harvard-Smithsonian Center for Astrophysics

M. C. WEISSKOPF, R. F. ELSNER,[3] P. GHOSH,[3] AND W. DARBRO
NASA George C. Marshall Space Flight Center

AND

P. G. SUTHERLAND[1]
McMaster University

*Received 1980 May 1; accepted 1980 June 9*

## ABSTRACT

The first image of an X-ray burst was recorded with the HRI detector at the *Einstein* Observatory while observing the globular cluster Terzan 2. The burst was coincident with a persistent X-ray source located near the center of the cluster (thus confirming an earlier suggested identification) and reached a peak luminosity exceeding $L_x \sim 5 \times 10^{38}$ $(d/10 \text{ kpc})^2$. After a rapid rise to peak luminosity, a double-peaked spectral variation was observed over the next $\sim$20 s with anticorrelated changes in the apparent emission region radius and temperature derived from blackbody (and "modified" blackbody) spectral fits. A shell or disk geometry, which undergoes adiabatic expansion and contraction, may be implied for the burst emission region. Alternatively, Comptonization is required. We also show that the peak burst luminosity must exceed the Eddington limit.

*Subject headings:* clusters: globular — X-rays: bursts

## I. INTRODUCTION

Ever since their discovery (Grindlay *et al.* 1976), X-ray burst sources have had a special relationship with the class of X-ray sources found in globular clusters. Six of the eight known globular cluster sources (Grindlay 1979) have been identified (see, e.g., Lewin and Clark 1979) as bursters. Two classes of models have been proposed to account for the bursts themselves: (1) instabilities in accretion onto a magnetized neutron star (Lamb *et al.* 1977; Baan 1977; Liang 1977*a*, *b*) or a black hole (Grindlay 1978*a*); or (2) thermonuclear flashes on neutron stars (Woosley and Taam 1976; Maraschi and Cavaliere 1977) which possibly require a helium shell (Joss 1978). Time-resolved spectra of bursts (e.g., Swank *et al.* 1977) have established that most Type I bursts (Hoffman, Marshall, and Lewin 1978) are well-fitted during their exponential decay by blackbody models of approximately constant radius (van Paradijs 1978) but decreasing temperature. However, it has generally not been possible to record continuum spectral variations within the burst maxima (but see Hoffman *et al.* 1979); such variations could restrict the burst models and geometry.

We report observations from the *Einstein* X-ray Observatory of a single burst and the associated persistent emission X-ray source in the globular cluster Terzan 2. The observations include the first direct image of an X-ray burst, which locates the source near the center of the globular cluster, and time-resolved (2.56 s) spectra which suggest that the burst emission may be either Comptonized or from a mass shell or disk whose radius changes during the first $\sim$20 s of the burst.

[1] Alfred P. Sloan Foundation Fellow.

[2] On leave from Polish Academy of Sciences, N. Copernicus Astronomical Center.

[3] NAS/NRC Resident Research Associates.

## II. OBSERVATIONS

The globular cluster Terzan 2 (Terzan 1971) was observed with the High Resolution Imager (HRI) and Monitor Proportional Counter (MPC) detectors at the *Einstein* X-ray Observatory (Giacconi *et al.* 1979) for $\sim$30 minutes on 1979 March 5 so that the identification (Grindlay 1978*b*) of both a bursting source and a persistent X-ray source (XB 1722−30 = 4U 1724−30 as reported by Swank *et al.* 1977 and Forman *et al.* 1978) with Terzan 2 could be tested. The identification was confirmed when both a burst source and a persistent source were observed to be coincident and within the globular cluster.

### *a) Imaging Data (HRI)*

In Figure 1 (Plate L11) we show the HRI image obtained in $\sim$30 s integrations immediately before (*a*), during (*b*), and after (*c*) the burst, together with the superposition (*d*) of the X-ray position on a deep-plate (IV-N, or near-IR) image of Terzan 2 (Grindlay 1978*b*). The full $25' \times 25'$ HRI field of view is shown, and the image size is $\sim 4''$ FWHM, or consistent with a single point source at $\alpha_{1950} = 17^h24^m19^s.8$, $\delta_{1950} = -30°45'39''.9$.

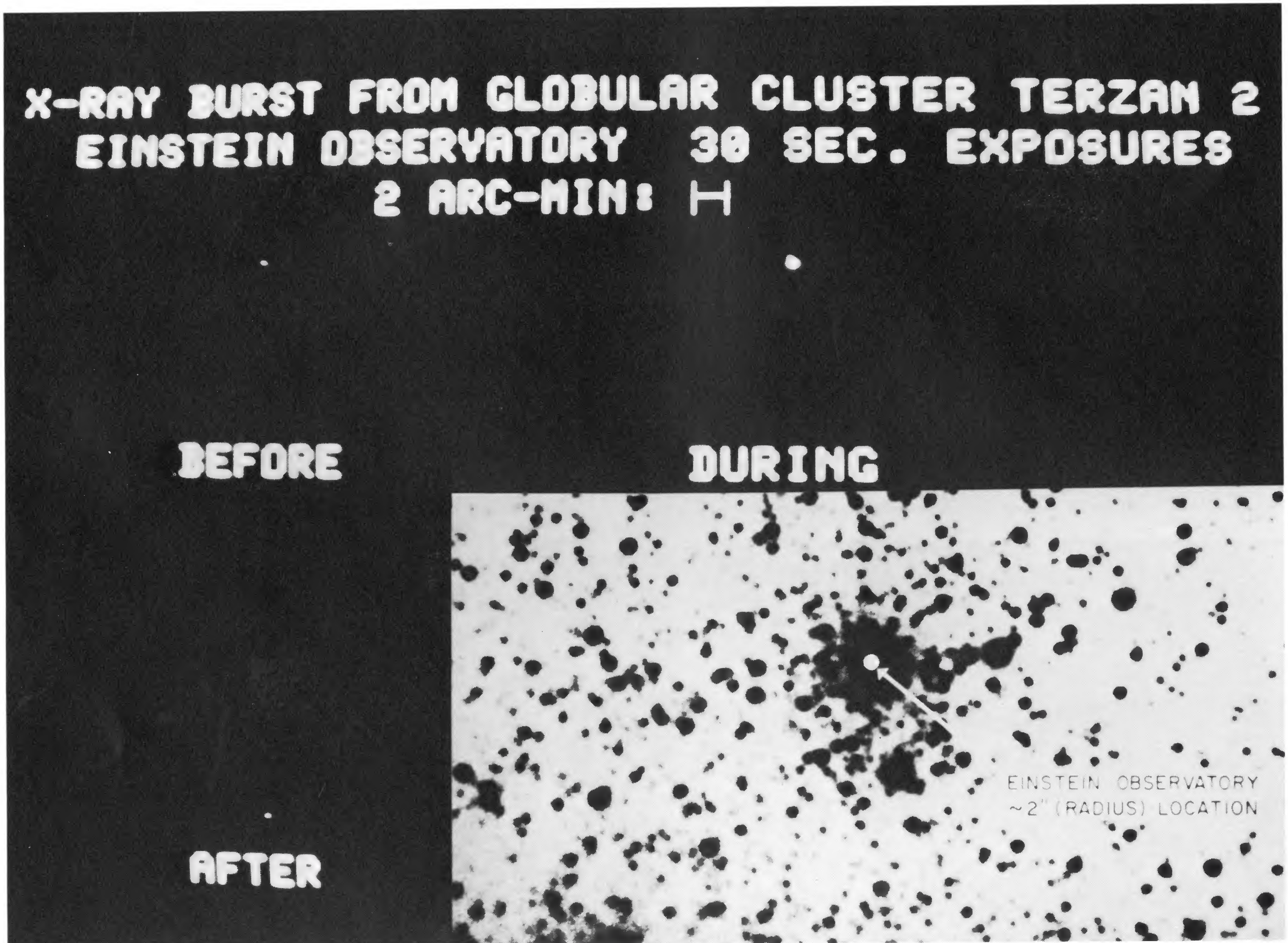


FIG. 1.—X-ray images of Terzan 2 before (*a*), during (*b*), and after (*c*) the X-ray burst. All exposures are 30 s. The X-ray position is superposed (*d*) on a deep near-IR image (CTIO 4 m IV-N plate) of the globular cluster (see text).

GRINDLAY *et al.* (*see* page L121)

This is 1″.6 ± 2″ from the center of Terzan 2, or at 0.23 ± 0.29 times the ~7″ core radius (Grindlay *et al.* 1980). There is no difference (<2″, at 90% confidence limit) in the position of the point source in Figures 1*a*–1*c*, indicating that the burster source and the persistent source are most probably one and the same object and that only one X-ray source is detected in the cluster core (see Grindlay *et al.* 1980 for the probability and implications of this conclusion).

Spectral data are not available for the HRI images, so the total luminosity can be estimated only for an assumed spectrum (determined here by the MPC—see below). Since the effective bandpass of the HRI is ~0.3–3 keV, it is much more sensitive to the low-energy cutoff and effective column density $N_H$ than is the MPC. The approximate agreement between the HRI count rate for the persistent source (0.22 ± 0.014 counts s$^{-1}$) and that (0.14 [+0.04, −0.01]) predicted from the MPC is therefore consistent with MPC spectral analysis. The HRI count-rate data during the burst indicate a burst onset time of 13:33:13.8 ± 0.3 UT, a rise time of $\lesssim$0.5 s, and a possible double-peaked intensity maximum (with ~4 s separation), followed by an exponential decay (with $\tau \sim 12$ s). A very different burst profile is seen by the MPC at higher energies.

### *b) Spectral Data and MPC Description*

In Figure 2 we show the count rate recorded by the MPC during the first ~400 s of the Terzan 2 observation. The total count rate in the 1.1–21 keV band at the burst peak (Fig. 2*a*) is comparable to that observed during MPC observations of the Crab. The energy-dependent burst profile is evident in the spectral channel groups plotted in Figures 2*b*–2*e*. The burst rise time is measured (by the MPC-TIP; see below) to be 0.25 ± 0.05 s, and the intensity maximum appears double peaked (with separation ~10 s) at hard energies. The onset time can be accurately measured (by the TIP) only in the full 1.1–21 keV energy range and is 1.8 ± 0.3 s *earlier* than that seen by the HRI. Thus the initial burst onset is relatively hard but rapidly softens. The burst decay (~20 s later), however, is soft with exponential time scales of ~12 s (first 20 s), ~40 s (next 100 s), and ~300 s (next ~500 s).

Before discussing the MPC spectral fits and timing studies in detail, we must first describe the MPC and analysis techniques used in this and forthcoming studies using MPC data from the *Einstein* Observatory. The MPC is a sealed, Argon-filled proportional counter (~667 cm$^2$ active area) with 1.5 mil Be windows and a 43′ (FWHM) field of view co-aligned with the telescope to within $\lesssim$1′. The total energy range (1.10–21.0 keV) is divided logarithmically into eight pulse-height analysis (PHA) channels. The spectral data are available every 2.56 s together with four background event registers. One of these, the coincidence rate, is least dependent on the spectral parameters of the X-ray source being observed but is very sensitive to the local particle background, which, in turn, is responsible for most of the variable background detected in the eight PHA channels. The good correlation between coincidence rate and detected background enables the background to be predicted as discussed below. Finally, the Time Interval Processor (TIP) circuitry of the MPC gives photon arrival times to within 10 $\mu$s or 1.6% of the time interval, whichever is larger, for a count-rate dependent fraction of all events in all eight PHA channels. Thus no energy information is available from the TIP data, and 2.56 s gaps in the TIP data (for memory readout) are introduced with increasing frequency as the total count rate rises above ~30 counts s$^{-1}$. A complete description of the MPC instrumentation is given by Gaillardetz *et al.* (1978).

The spectral fits to MPC data are derived by minimizing the $\chi^2$ deviation between the observed spectrum (background subtracted) and tables of count-rate spectra which are precalculated for fixed ranges of spectral index or temperature and low-energy absorption. The background in each of the eight PHA channels is predicted every 2.56 s by using the current value of the coincidence rate and the spatially dependent correlation (derived from time-ordered background maps) between the coincidence and PHA rates. Using the asymptotically constant background (~17 counts s$^{-1}$) data only, background, and thus source fluxes can be determined in a typical ~1000 s observation with 1 $\sigma$ uncertainty ~0.3 counts s$^{-1}$ (~0.2 UFU).

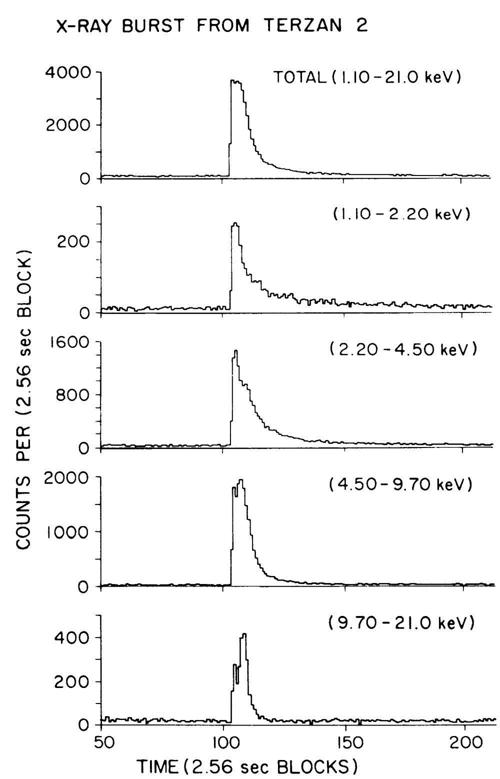


FIG. 2.—X-ray burst from the globular cluster Terzan 2 as recorded by the MPC.

## III. SPECTRAL AND TEMPORAL ANALYSIS RESULTS

As can be seen in Figure 2, the Terzan 2 burst shows marked spectral variability. We have fitted the PHA data before, during, and after the burst to five spectral shapes: power law, exponential, bremsstrahlung, blackbody (BB), and modified blackbody (MBB). The latter accounts for the scattering opacity modification of a blackbody and is taken from the approximate form given by Swank, Eardley, and Serlemitsos (1979). Before and after ($\gtrsim 100$ s) the burst, the persistent source is best described (reduced $\chi^2 = 1.1$) by a bremsstrahlung spectrum with $kT = 8.6 \pm 0.3$ keV, $N_{\mathrm{H}} \approx 7 \pm 2 \times 10^{21}$ cm$^{-2}$, and $L_x \approx 6 \times 10^{36} d_{10}^2$ ergs s$^{-1}$. During the first $\sim$20 s of the burst, BB models fit best (reduced $\chi^2 = 1.5$ vs. 3.3 for MBB and $\gtrsim 100$ for bremsstrahlung). In Figure 3 we plot the total apparent burst luminosity $L_a$, hardness ratio, low-energy absorption column density $N_{\mathrm{H}}$, apparent radius $R_a$, and temperature $T_a$ values versus time for the BB fits. For an underlying source mass $M$, these apparent quantities are related by the gravitational redshift factor $g = (1\text{-}2GM/c^2R)^{1/2}$ to the true values: $L_a = g^2L$, $R_a = g^{-1}R$, $T_a = gT$. A striking double-peaked variation during the first $\sim$30 s of the burst is evident for all these quantities (except $N_{\mathrm{H}}$) for both the BB and MBB fits. The $N_{\mathrm{H}}$ variation, and particularly the approximately constant but low value during the first $\sim$13 s of the burst, can be reconciled with the larger quiescent source value (which is consistent with being entirely interstellar, given the optical-IR extinction of $A_v \sim 3$–4 [Grindlay 1978*b*; Malkan, Kleinman, and Abt 1980], and would give significantly worse $\chi^2 \sim 3.0$) if there is an additional soft spectral component just after burst onset. This is, in fact, suggested by an apparent excess in the two lowest-energy channels (1.10–2.20 keV) above the best-fit BB spectra during the first $\sim$10 s. The HRI count rate is also consistent with a soft excess, but there is not sufficient (MPC) spectral resolution to determine uniquely the spectral shape or fractional luminosity in this soft component. Similar evidence for a soft excess after burst onset has been found in MPC observations of 4U 1636−53 (Marshall and Grindlay 1980).

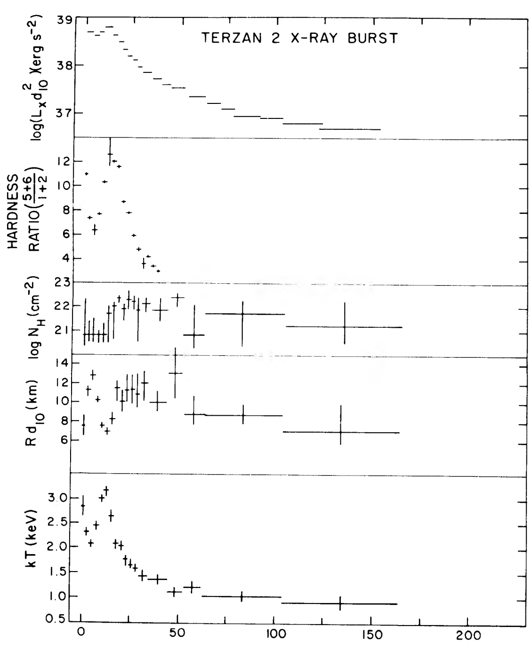


FIG. 3.—Profiles (2.56 s bins) of best-fit blackbody luminosity ($\propto R^2T^4$), hardness ratio [ratio of fluxes (4.5–9.7 keV)/(1.1–2.2 keV)], approximate low-energy absorption column density $N_{\mathrm{H}}$, blackbody radius $R$, and temperature $kT$ of Terzan 2 X-ray burst (see text). Error bars are shown for only three points for the hardness ratio but for all points for $N_{\mathrm{H}}$, $R$, and $kT$.

The apparent radius determined from the BB fits changes during the burst peak from $\sim 7d_{10}$ to $\sim 13d_{10}$ km in a double-peaked fashion. (Note that since the distance to Terzan 2 has been estimated to be 7 kpc [Grindlay 1978*b*] or 14 kpc [Malkan, Kleinman, and Abt 1980], we may take the distance to be $\sim$10 kpc and $d_{10} \sim 1$.) A monotonic decrease of apparent radius back to $\sim 7d_{10}$ km is also evident during the burst decay. A similar but much larger range of decreasing apparent radius (from $\sim 100d_{10}$ km to $\sim 15d_{10}$ km) was observed during the decay of the longer-duration burst observed from this source by the *OSO 8* satellite (Swank *et al.* 1977).

High time resolution studies of the burst maximum and decay using the TIP data reveal no significant fast fluctuations or periodicities in the broad-band range 1.1–21 keV. Folding analyses were conducted for all independent periods as short as 1 ms, and upper limits (90% confidence) for the pulsed fraction of $\sim$8% (for a sinusoidal pulse shape) were obtained for the burst maximum and $\sim$15% for the decay. For the persistent source, upper limits of $\gtrsim$25% fractional pulsed flux were obtained for stable pulsations with periods $\sim$1 ms–100 s.

## IV. DISCUSSION AND CONCLUSIONS

Although double-peaked structure in burst intensity (Lewin *et al.* 1976) and temperature (Hoffman *et al.* 1979) have been reported, the time-resolved burst spectra presented here are the first to show double-peaked changes in both apparent radius $R$ and temperature $T$ wherein $R$ and $T$ are anticorrelated. We shall briefly discuss two possible interpretations which, though not unique, have interesting consequences.

As Figure 4 shows, the $R_a$ versus $T_a$ variation of the first eight points (20.48 s) suggests the simple relation $TR^\beta$ = constant. This relation, and the fact that $\beta \sim 0.67$ best describes the data, suggests that the burst emission region may be an adiabatically expanding (and contracting) shell or disk with volume $V \sim R^2$ (and approximately constant thickness) since then the adiabatic condition $TV^{\gamma-1} = TV^{\beta/2}$ = constant gives $\gamma \sim 4/3$, as expected for gas dominated by radiation energy density (note that $\gamma \sim 5/3$ would require an unlikely "linear" geometry $V \sim R$). The observed $T$ versus $R$ relation could also arise from a variation in the Compton scattering of a BB burst spectrum in a constant volume since then photon number (not energy) is conserved and $T^3R^2$ = constant.

The adiabatic shell (or disk) picture allows the density in the emission region to be estimated. We note that the changes in the emission volume occur on time scales ($\sim$5 s) long compared with local sonic times or free-fall times for accretion onto a neutron star or black hole. Thus the emission region changes in a quasi-static manner and there may be approximate equipartition between the radiation energy density and gravitational energy density (it will follow that thermal pressure is negligible). In this case, the matter density in the emitting region of the apparent radius $R_a \sim 10$ km and temperature $T_a \sim 3 \times 10^7$ K is $\rho \sim \sigma R_a T_a^4/cGMg^3 \sim 2 \times 10^{-5}$ g cm$^{-3}$, where $\sigma$ is the Stefan Boltzman constant and we take $M \sim 1.4\ M_\odot$. This corresponds to an effective particle density of $n_H \sim 2 \times 10^{19}$ cm$^{-3}$ in the emitting shell or disk and suggests that the source is optically thick to electron scattering if its characteristic thickness is $\gtrsim$0.8 km, or only $\sim$10% of the apparent change in radius. Thus electron scattering may be important and could modify the values derived from the "adiabatic" BB model. More accurate MBB model spectra (than the Swank *et al.* model used here) might then better fit the data. Our density estimate is consistent with either expansion of a neutron star "photosphere," as in the nuclear flash model (Joss 1978), or with contraction (approximately free-fall from $R \sim 10^9$ cm to $R \sim 10^6$ cm) of an accretion shell with density $n \sim 10^{15}$ cm$^{-3}$, as in an accretion instability model (e.g., Grindlay 1978*a*).

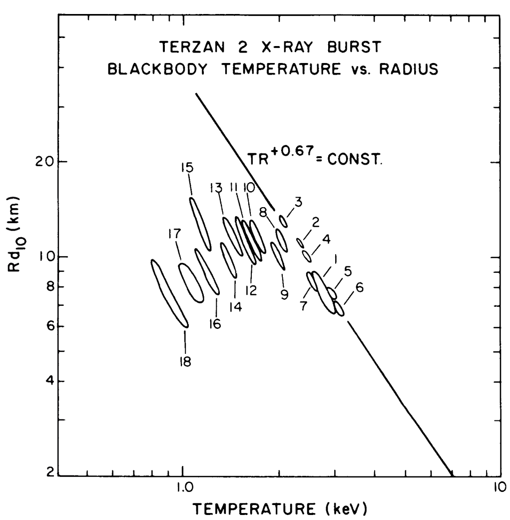


FIG. 4.—Blackbody temperature vs. radius for X-ray burst from Terzan 2. The 68% (1 $\sigma$) confidence ellipses are shown for each 2.56 s integration after burst onset in the time order given by the numbers. Points 1-8 may suggest either adiabatic changes of a shell (or disk) emission region or Comptonization of the underlying source; points 9–18 (and Fig. 3) show that the burst decay is well described by a cooling blackbody source of decreasing radius.

The Comptonization hypothesis could account for the two peaks of apparent radius and temperature from scattering or radiative transfer effects in the radiating shell or disk. Photon diffusion out from a central source into a surrounding disk might give rise to the double-peaked structure as a Compton echo. Alternatively, a decrease in opacity of a surrounding mass shell may result from Compton heating by the (initially) hard burst; reradiation by the shell then gives the second peak. Compton heating or cooling of an accretion flow by the initial burst peak will also give multiple peaks (Lamb *et al.* 1977; Grindlay 1978*a*).

Interesting limits for the source mass and radius can be derived from the BB fits and observed peak temperature (see also Marshall 1980). Expressing the luminosity as a factor $k$ times the local Eddington luminosity [$(1.3 \times 10^{38})\ (M/M_\odot)\ g^{-1}$ ergs s$^{-1}$], we obtain an implicit relation between the source mass and true radius, $M \propto (1/k)T_a^4R^2/g^3(M, R)$, where $g$ is again the gravitational redshift factor. Thus a given value of the apparent blackbody temperature and a given $M$ and $R$ value give the corresponding value of $k$. For possible neutron-star values of $M$ and $R$ (i.e., $\sim$1.4 $M_\odot$ and $\sim$7 km), the Terzan 2 burst then requires $k \sim 10$ at the burst maximum (where $T_a \sim 3 \times 10^7$ K), and is thus inconsistent with a blackbody emitting at the Eddington limit as expected in flash models (Joss 1978). It appears likely (Marshall 1980) that $k \gtrsim 10$ at some point during the burst for any values of $M$ and $R$ from neutron-star models or for black holes with $M \gtrsim 1\ M_\odot$.

This work was partially supported by NASA contract NAS8-30751. We thank Don Lamb and George Rydicki for useful discussions.

## REFERENCES


Baan, W. A. 1977, *Ap. J.*, **214**, 245.

Forman, W., Jones, C., Cominsky, L., Julian, P., Murray, S., Peters, G., Tananbaum, H., and Giacconi, R. 1978. *Ap. J. Suppl.*, **38**, 357.

Gaillardetz, R., Bjorkholm, P., Mastronardi, R., Vanderhill, M., and Howland, D. 1978, *IEEE Trans Nucl. Sci.*, *NS*-**25**, 437.

Giacconi, R., *et al.* 1979, *Ap. J.*, **230**, 540.

Grindlay, J. E. 1978*a*, *Ap. J.*, **221**, 234.

———. 1978*b*, *Ap. J.* (*Letters*), **224**, L107.

———. 1979, in *Galactic X-Ray Sources* (Proc. NATO ASI, Cape Sounion, Greece), ed. P. W. Sanford (London: Cambridge University Press), in press.

Grindlay, J., Gursky, H., Schopper, H., Parsignault, D. R., Heise, J., Brinkman, A. C., and Schrijver, J. 1976, *Ap. J.* (*Letters*), **205**, L127.

Grindlay, J., Hertz, P., Murray, S., and Lightman, A. 1980, in preparation.

Hoffman, J. A., Marshall, H. L., and Lewin, W. H. G. 1978, *Nature*, **271**, 630.

Hoffman, J. A., *et al.* 1979, *Ap. J.* (*Letters*), **233**, L51.

Joss, P. C. 1978, *Ap. J.* (*Letters*), **225**, L123.

Lamb, F., Fabian, A., Pringle, J., and Lamb, D. 1977, *Ap. J.*, **217**, 197.

Lewin, W. H. G., and Clark, G. 1979, in *Galactic X-Ray Sources* (Proc. NATO ASI, Cape Sounion, Greece), ed. P. W. Sanford (London: Cambridge University Press), in press.
Lewin, W., Hoffman, J., Doty, J., Hearn, D., Clark, G., Jarnigan, J., Li, F., McClintock, J., and Richardson, J. 1976, *M.N.R.A.S.*, **177**, 83P.
Liang, E. P. T. 1977*a*, *Ap. J.* (*Letters*), **211**, L67.
———. 1977*b*, *Ap. J.*, **218**, 243.
Malkan, M., Kleinman, D., and Abt, J. 1980, *Ap. J.*, in press.
Maraschi, L., and Cavaliere, A. 1977, *Highlights of Astronomy*, Vol. **4**, Part I, ed. E. A. Muller (Dordrecht: Reidel), p. 127.
Marshall, H. 1980, in preparation.
Marshall, H., and Grindlay, J. 1980, in preparation.
Swank, J., Becker, R., Boldt, E., Pravdo, S., and Serlemitsos, P. 1977, *Ap. J.* (*Letters*), **212**, L73.
Swank, J., Eardley, D., and Serlemitsos, P. 1979, *Ap. J.* (*Letters*), submitted.
Terzan, A. 1971, *Astr. Ap.*, **12**, 477.
van Paradijs, J. 1978, *Nature*, **274**, 650.
Woosley, S. E., and Taam, R. E. 1976, *Nature*, **273**, 101.

J. E. Grindlay, P. Hertz, H. L. Marshall, and A. Soltan: Harvard-Smithsonian Center for Astrophysics, 60 Garden Street, Cambridge, MA 02138

W. Darbro, R. F. Elsner, P. Ghosh, and M. C. Weisskopf: NASA George C. Marshall Space Flight Center, Code ES62, Marshall Space Flight Center, AL 35812

P. G. Sutherland: Department of Physics, McMaster University, 1860 Main Street, West Hamilton, Ontario L8S 4M1, Canada